Quantitative investigation of the influence of carbon surfactant on Ge surface diffusion and island nucleation on Si(100)

G. M. Vanacore,[1] M. Zani,[1] G. Isella,[2] J. Osmond,[2,3] M. Bollani,[2] and A. Tagliaferri[1]
[1]*CNISM and Dipartimento di Fisica, Politecnico di Milano, Piazza Leonardo da Vinci, 32-20133 Milano, Italy*
[2]*CNISM and LNESS, Dipartimento di Fisica, Politecnico di Milano, Polo Regionale di Como, Via Anzani 42, 22100 Como, Italy*
[3]*Institute of Photonics Sciences, 08860 Barcelona, Spain*
(Received 8 June 2010; published 30 September 2010)

We investigated the surface diffusion and island nucleation of Ge on Si(100) in presence of a submonolayer coverage of carbon as surfactant by using scanning Auger microscopy and atomic force microscopy. Ge stripes have been deposited and lithographically etched on a Si substrate and used as sources for the surface diffusion of Ge promoted by annealing at 600, 650, and 700 °C. The diffusion coefficient has been determined by fitting the postannealing coverage profiles measured by Auger microscopy with a one-dimensional continuous model. The carbon coverage has been spatially modulated on a single sample, allowing the measurement of the diffusion coefficient as a function of the C thickness at 600 °C. We show that the reduction in the diffusion coefficient while increasing the surfactant coverage is described by a linear dependence of the diffusion activation energy on the C coverage. This dependence is discussed in terms of the chemical interactions among Si, C, and Ge, of the surface roughness and the local strain field induced by the C surfactant. Spontaneous nucleation of SiGe islands coexists with the continuous surface diffusion of Ge. The transition of the island nucleation as a function of the carbon coverage is observed to be continuous from the Stranski-Krastanov mode to the Volmer-Weber regime. We propose a consistent scenario correlating diffusion and nucleation parameters within a diffusion limited growth regime and show the existence of a threshold for C coverage below which no effect is observed.

DOI: 10.1103/PhysRevB.82.125456 PACS number(s): 68.35.Fx, 81.16.Dn, 68.55.ag, 68.37.−d

I. INTRODUCTION

Growth of Ge on Si surfaces has attracted much attention because of its importance for both the semiconductor technology and the understanding of fundamental physical processes. The formation of self-assembled SiGe islands is strongly dependent on the surface-diffusion coefficient of Ge and Si atoms, which is rapidly varying with the temperature[1,2] and submonolayer amounts of surface impurities.[3]

The surface diffusion of Ge on Si(100) follows an anisotropic Arrhenius behavior[4] due to the (2×1) reconstruction with dimer rows forming on the (100) surface. The surface mass transport has been experimentally studied both by directly measuring the diffusion length on a macroscopic scale (about 10^{-3} m)[5] and by monitoring on a microscopic scale the temperature dependence of the width of islands free zones around preferential nucleation sites.[4,6,7] Activation-energy barriers (0.6–1.2 eV) and diffusion coefficients (10^{-9}–10^{-8} cm^2/s at 600 °C) have been theoretically obtained by using molecular-dynamics simulations[8,9] and *ab initio* calculations.[10]

The surface diffusion, and more generally the growth mode of Ge on Si, can be controlled by using surface-active species (surfactants)[11,12] that strongly modifies the surface free energy of both Ge and Si.[13] Tromp and Reuter[14] showed that As and Sb surfactants are energetically driven to float at the surface during growth, thus providing a large driving force for the Ge atoms to incorporate into the surface, which can suppress the surface diffusion and prevent island formation. An opposite behavior is expected when carbon is used as a surfactant with the repulsive chemical interaction between Ge and C atoms[15] forcing carbon into the shallow layers of the substrate.[16] Thus Ge atoms lie in the top layer on the rough and strained interfaces created by the underlying C-rich layers and the diffusion coefficients are strongly affected.

Another important process typical of lattice-mismatched systems is the island nucleation driven by the elastic relaxation of the strain. Indeed, using a surfactant can enhance island formation by modifying the energy and the strain state of the surface, and the idea of controlling shape, size, and density of self-assembled islands has been already reported.[17,18]

A recent bottom-up strategy toward the engineering of the self-assembly process of Ge islands involves the use of carbon as a surfactant. The growth of C-induced SiGe islands has been extensively studied[3,19–23] for the possibility to tailor their properties for potential application in nanoscale devices.[24] The growth mode of Ge on a Si(100) surface precovered with a submonolayer amount of carbon, generating $c(4\times4)$ reconstructed domains, has been studied by Stoffel *et al.*,[25] showing that the growth proceeds via a Volmer-Weber (VW) mode. This growth mode has been observed also by Leifeld *et al.*[26] using scanning tunneling microscopy and by Dentel *et al.*[23] and Bernardi *et al.*[27] through reflection high-energy electron diffraction studies. However, the microscopic mechanism of surfactant effect upon the growth process evolution is still under investigation and the identification of the microscopic factors governing the relative growth of individual nanostructures is an important issue that still needs to be addressed for a complete understanding of the process. Bernardi *et al.*[28] recently demonstrated that by deposing a carbon layer over a SiGe buffer layer it is possible

to manipulate the epitaxial growth of Ge dots in a kinetically limited deposition regime. In comparison with Ge islands directly grown on a bare Si surface, the average size of the C-induced Ge dots is generally smaller and the island density is larger.[29,30] This is usually attributed to a decrease in diffusion length of adatoms on a C precovered surface,[31] even if a direct experimental demonstration of such a reduction in the Ge diffusion induced by the C surfactant is still lacking.

In this paper, we quantitatively study how a controlled carbon coverage influences the thermal surface diffusion and nucleation of Ge atoms on the Si(100) surface. The use of lithographically defined Ge stripes as sources of diffusion allows for a direct measurement of the long- and short-range diffusion parameters at the same time. We have directly determined the diffusion coefficients on a microscopic scale and by monitoring *in situ* both the diffusion process and the island self-organization we have investigated the influence of the surface atomic mobility on the growth evolution.

First we discuss the temperature dependence of the diffusion coefficient on a C-free Si surface at 600, 650, and 700 °C. Then a quantitative correlation of the diffusion parameters at 600 °C with the carbon coverage in the submonolayer regime is obtained by monitoring the Ge diffusion on a Si surface precovered with a spatially modulated C coverage. We experimentally show that the diffusion coefficient at 600 °C presents a strong dependence on carbon coverage. To understand the origin of this dependence we critically discuss the role played by the chemical interactions among Si, C, and Ge and by the surface roughness and local strain field induced by the C surfactant. By coupling scanning Auger microscopy (SAM) and atomic force microscopy (AFM) analysis the critical overlayer (OL) thickness for nucleation has been extracted, showing a continuous transition from 3 ML down to fractions of ML as a function of carbon coverage. This gives the experimental evidence of a C-induced continuous transition from the Stranski-Krastanov (SK) growth mode, where a two-dimensional (2D) wetting layer is formed before the three-dimensional (3D) nucleation, to the Volmer-Weber growth regime, with leading to a direct formation of 3D islands without wetting layer. Moreover we show that the experimental behavior of the nucleation as a function of the C coverage is fully consistent with the diffusion parameters, that have also been determined experimentally, within a scenario where the surface diffusion is indirectly determined by carbon, due to the strain induced in the substrate by intermixing with Si in its shallow layers. Finally, size and density of spontaneously nucleated SiGe islands have been monitored in areas with different carbon coverage and have been directly correlated with the Ge surface atomic mobility. We propose that the growth process evolution can be primarily interpreted within a diffusion-limited regime.

II. EXPERIMENT AND METHOD

The samples consist of Ge stripes (width $\sim 3-5$ μm) obtained by a photolithographic patterning of pure Ge thin films (thickness ~ 50 nm), grown on a Si(100) substrate by low-energy plasma-enhanced chemical vapor deposition.[32] Removal of native silicon oxide and germanium oxide has been obtained by using a diluted HF solution at 10% for 30 s at room temperature. Surface contaminations have been removed by *in situ* low-temperature out-gassing ($T \leq 500$ °C) and Ar^+ ion sputtering. The ions were accelerated to 4 keV kinetic energy with a beam current of ~ 0.4 μA; the ion beam had a spot size of about 0.5×1 mm^2 and has been rastered over an area of 10×10 mm^2 (greater than the whole sample surface), hitting the sample with a take-off angle of 30°. A PHI 660 SAM has been used for a spatially resolved chemical characterization of the samples.

To investigate the surface diffusion in presence of carbon, we exploited the presence of C and O on the Si surface due to adsorption of CO, CO_2, and carbon hydrogenates, as revealed by Auger analysis performed after the insertion of the sample in the vacuum system. A pure carbon layer has been then obtained by an *in situ* low-temperature out-gassing. In fact, a several minutes long out-gassing performed at 500 °C results in a complete O desorption leaving a C layer on the surface. No residual oxygen was observed within the detection sensitivity limit of 1%. The residual carbon layer has been reproducibly found on several samples after the out-gassing. Hydrogen contamination, undetectable with the Auger probe, is reasonably eliminated during the out-gassing.[33]

The stripes act as Ge sources directly placed on the sample surface and a continuous diffusion profile is obtained after annealing at high temperatures (600, 650, and 700 °C) in UHV (see Sec. III A). Moreover, self-assembled SiGe islands spontaneously originate along the diffusion profile (see Sec. III C).

The samples have been annealed by Joule heating running a dc through the Si substrate. The temperature stabilization takes less than 30 s, and the temperature spatial distribution is highly uniform in the investigated area, as demonstrated by the reproducibility of the diffusion profiles measured in different zones of the sample surface. The base pressure during the annealing time was always better than 1×10^{-9} torr.

To characterize *in situ* the Ge diffusion profiles and the thickness of the carbon layer, we have monitored the intensities of Ge LMM (~ 1150 eV), Si LMM (~ 90 eV), Si KLL (~ 1610 eV), and C KLL (~ 270 eV) Auger lines as a function of distance from the Ge stripe. The AFM data have been obtained by a Veeco Innova microscope, operated in tapping mode with ultrasharp tips (nominal tip radius about 2 nm), to analyze *ex situ* the nucleated islands. To extract quantitative information a statistical analysis of AFM data has been performed on about 500 islands using freely available software tools.[34]

III. RESULTS AND DISCUSSION

A. Surface diffusion on a C-free Si(100) surface

During the annealing process the Ge moving from the stripe diffuses on the Si surface forming a continuous OL. Figure 1(a) shows the scanning electron microscopy (SEM) micrograph of the stripe before (upper inset) and after (main panel) a 10 min annealing at 600 °C. Before the annealing the surface contaminants have been completely removed by using an *isotropic* ion sputtering. After annealing, surface roughness was about 0.2 nm as determined by AFM analysis.

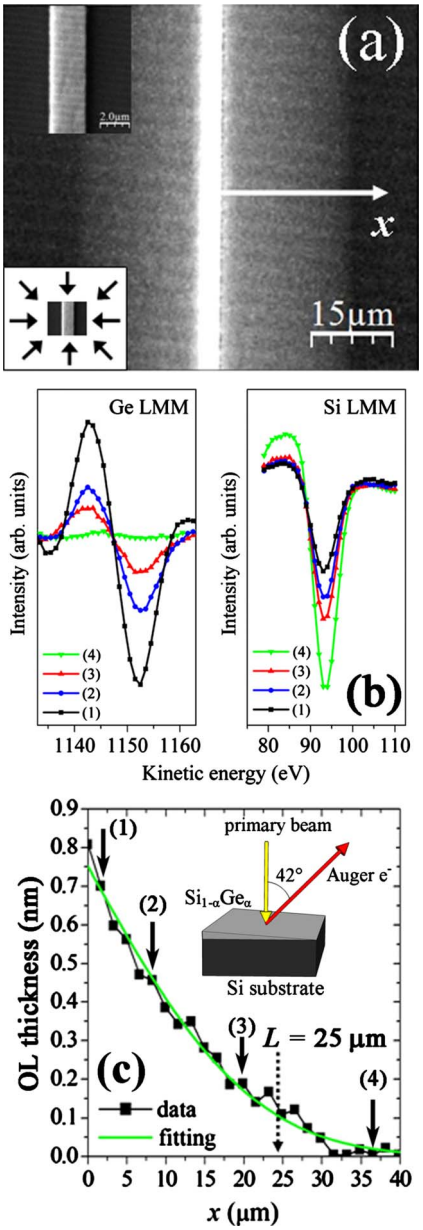

FIG. 1. (Color online) (a) SEM image of the stripe after annealing at 600 °C for 10 min showing a bilateral diffusion (gray shaded area). Surface contaminations have been removed by using an isotropic ion sputtering (as schematically shown in the inset in the bottom-left corner). In the top-left corner is shown the SEM image of the stripe before the annealing. (b) Ge LMM and Si LMM Auger lines measured at different distances from the stripe as indicated by the solid black arrows in the panel (c). (c) Overlayer thickness as a function of the distance from the source as determined by SAM analysis (black squares). The green continuous line is the best fitting of the experimental data using the analytical solution of a 1D diffusion model (see text). Inset: schematic of the detection geometry and of the diffusion region as represented inside the discrete layer model.

The shading at the sides of the stripe in Fig. 1(a) result from the compositional contrast of the secondary electron emission between Ge, diffused on the surface, and Si in the substrate. Spatially resolved Auger analysis allowed to measure the thickness and composition of the OL along the diffusion profile as a function of the distance, x, from the stripe. Figure 1(b) shows the Ge LMM and Si LMM Auger lines measured at different distances from the stripe after a 10 min annealing at 600 °C and Fig. 1(c) represent the corresponding OL behavior. The determination of the OL thickness has been obtained by fitting the Ge LMM and Si LMM Auger line intensities (kinetic energy of 1150 and 90 eV) measured as a function of x with a discrete layer model[35] where the OL is approximated by a $Si_{1-\alpha}Ge_{\alpha}$ thin film of variable thickness and uniform composition α. Within this discrete layer model the normalized Si LMM and Ge LMM Auger line intensities are given by the following relations:

$$\frac{I_{Si}}{I_{Si}^{STD}}(x) = [1-\alpha(x)]\frac{(n_V)_{Ge}}{(n_V)_{Si}}\left\{1-\exp\left[-\frac{h(x)}{\lambda_{Si}\cos\delta}\right]\right\} + \exp\left[-\frac{h(x)}{\lambda_{Si}\cos\delta}\right], \quad (1a)$$

$$\frac{I_{Ge}}{I_{Ge}^{STD}}(x) = \alpha(x)\left[1-\exp\left(-\frac{h(x)}{\lambda_{Ge}^{SiGe}\cos\delta}\right)\right], \quad (1b)$$

where h is the overlayer thickness, I_{Ge}^{STD} and I_{Si}^{STD} are the standard intensities for bulk Ge and Si, respectively; $\lambda_{Ge}^{Si}=2.66$ nm,[36] $\lambda_{Ge}^{Ge}=2.16$ nm,[36] and $\lambda_{Ge}^{SiGe}=\alpha\lambda_{Ge}^{Ge}+(1-\alpha)\lambda_{Ge}^{Si}$ are the inelastic mean-free path (IMFP) for Ge LMM Auger electrons propagating in a Si, Ge, and SiGe matrix, respectively; $\lambda_{Si}=0.52$ nm (Ref. 36) is the IMFP for Si LMM Auger electrons (in this case the dependence from the matrix is negligible); n_V is the volume atomic density in the bulk materials (44.2 atoms/nm^3 for Ge and 49.9 atoms/nm^3 for Si); $\delta \approx 42°$ is the angle between the normal to the surface and the outgoing direction of Auger electrons collected by the energy analyzer [see inset in Fig. 1(c)].

The first term in Eq. (1a) is related to the contribution to the Si LMM intensity from Si intermixed inside the OL, while the second term accounts for the attenuation of the substrate signal due to the presence of the OL. Equation (1b) for the Ge LMM intensity contains only the term related to Auger electrons originated inside the overlayer [see inset in Fig. 1(c)]. The data analysis takes advantage of the following facts: (i) the Ge LMM Auger electrons bring information from the whole OL because their IMFP is greater than its maximum thickness and (ii) the Si LMM decay channel is more suitable than the Si KLL one for the investigation of the OL, because the Si LMM intensity is strongly affected by the OL thickness (Si LMM electrons have an IMFP five times shorter than the Si KLL ones[36]).

For the annealing at 600 °C an average Ge relative concentration of about 0.81 ± 0.05 has been found, in good agreement with the values found in literature for the case of molecular beam epitaxy (MBE) deposition.[37] The value of composition, as obtained by the discrete layer model, exhibits a relative dispersion between the several data sets of about 12%. This dispersion is comparable with (1) the uncertainty introduced by the physical quantities of the model (namely, the IMFPs, for which has been assumed an error of lower than 5%, which is commonly accepted) and (2) the possible

systematic errors induced by a gradient of the composition inside the overlayer along its depth. We have verified that, even in the extreme case of a triangular profile of the composition inside the OL, the mean composition predicted by the model lies within the dispersion boundaries.

The dependence of the OL thickness as a function of x [Fig. 1(c)] is attributed to the diffusive motion of the atoms from the source and can be well understood in the framework of an analytical one-dimensional (1D) diffusion model.[38] The model strictly applies for the case of negligible intermixing between the migrating species and the substrate atoms. The hypothesis is not strictly verified in the present case as we found a partial Si incorporation inside the overlayer from the Auger analysis (see above). Indeed, considering that the local atomic motion is fast compared with the Ge flux,[39] the Si intermixing occurs on a time scale much shorter than the diffusion motion of the Ge atoms from the stripe, and the model can be generalized by supposing that the Ge surface diffusion is mediated by Si incorporation inside the overlayer. The correspondent diffusion parameters obtained by the model are essentially related to a SiGe alloy with high Ge content, and we will refer to them as Ge effective diffusion parameters.

In the meaning given above, the Ge coverage h follows the one-dimensional diffusion equation,[38] according to which the gradient in the chemical potential induced by the difference of Ge concentration between the stripe and the surrounding regions is the driving force for the surface diffusion

$$\frac{\partial h}{\partial t} = D\frac{\partial^2 h}{\partial x^2}, \tag{2}$$

where t is time and D is the diffusion coefficient which depends on the temperature, T. By considering the geometry of our experiment $[h(x,t)=0$ for $t=0,\ x>0]$ and in the hypothesis of a constant height source $[h(x,t)=h_0$ for $x=0,\ \forall\ t\in[0,\tau]$, where τ is the annealing time], the Ge coverage along the diffusion profile is given by the following relation:[38]

$$h = h_0\left[1 - \mathrm{erf}\left(\frac{x - x_0}{L}\right)\right], \tag{3}$$

where x_0 is the position of the stripe edge and $L=2\sqrt{D\tau}$ is the diffusion length. The green continuous line in Fig. 1(c) is the best fitting of the experimental data using Eq. (3) for a 10 min annealing at 600 °C. The diffusion lengths represented in Fig. 2(a) were determined similarly for each couple of temperature and annealing time on data taken at three temperatures with several annealing times. Then the diffusion coefficient at each temperature is extracted by linearly fitting the $L^2/4$ values for each temperature in Fig. 2(a). They are shown in Fig. 2(b) as an Arrhenius plot of D, and the green line is the fitting of the data with the corresponding Arrhenius law

$$D = 6.08 \times 10^{-2}\ \exp\left(-\frac{1.24\ \mathrm{eV}}{K_B T}\right)\ \mathrm{cm}^2/\mathrm{s}. \tag{4}$$

The values found for the diffusion constant $D_0=6.08\times10^{-2}$ cm^2/s and for the activation energy $E_A=1.24$ eV are

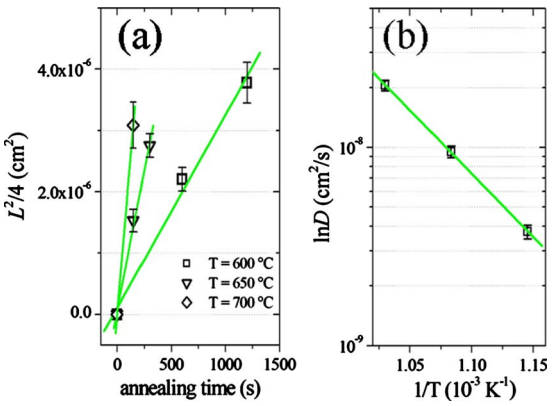

FIG. 2. (Color online) (a) $L^2/4$, with L diffusion length, plotted as a function of the annealing time, τ, for different temperatures (600, 650, and 700 °C). Linear fittings of the experimental data were used to extract the values of the diffusion coefficient, D, at different temperatures ($L^2=4D\tau$). (b) The diffusion coefficient has an exponential temperature dependence given by an Arrhenius law: diffusion constant $D_0=6.08\times10^{-2}$ cm^2/s, activation energy $E_A=1.24$ eV.

in good agreement with both the experimental[5,6] and theoretical[9,10] literature. A strong anisotropy of the surface diffusion has been experimentally demonstrated[4] and a theoretical model has been proposed,[9,10] where the diffusion parallel to the dimer rows, the *easy diffusion*, is characterized by an activation energy $E_A=0.73$ eV and a diffusion constant $D_0=4.3\times10^{-4}$ cm^2/s, and in perpendicular direction, the *hard diffusion*, by $E_A=1.17$ eV and $D_0=2.8\times10^{-3}$ cm^2/s.[9] We notice that in our setup Eq. (4) is used to describe the surface-mass transport over a length scale of a few tens of micrometers, which exceeds significantly the typical width of single terraces and of the dimer rows domains. Thus, the measured diffusion coefficient describes the diffusion averaged over both dimer orientations domains and across their boundaries.

B. Continuous surface diffusion on a C covered Si(100) surface

We discuss here the dependence of the Ge surface diffusion from the C coverage. In order to compare the effect of different coverages in the same environmental conditions, we have produced a carbon coverage varying continuously from zero to about few monolayers (MLs) along the direction y parallel to the stripe (see Fig. 3) according to the following procedure. A homogeneously carbon-covered surface has been obtained as described in the experimental section (Sec. II). Then the surface has been ion sputtered while a shutter, having an edge perpendicular to the stripe and parallel to the sample surface, was moved along the y direction. This allowed the exposure of an increasing portion of the surface with time. In this case the sputtering direction has been kept fixed with projection along x (instead of using the isotropic bombardment adopted before) in order to exploit the shutter motion. As a side effect, the C film is not removed from the area shadowed by the stripe (the right side of the stripes shown in Fig. 3). The C coverage before Ge diffusion as a

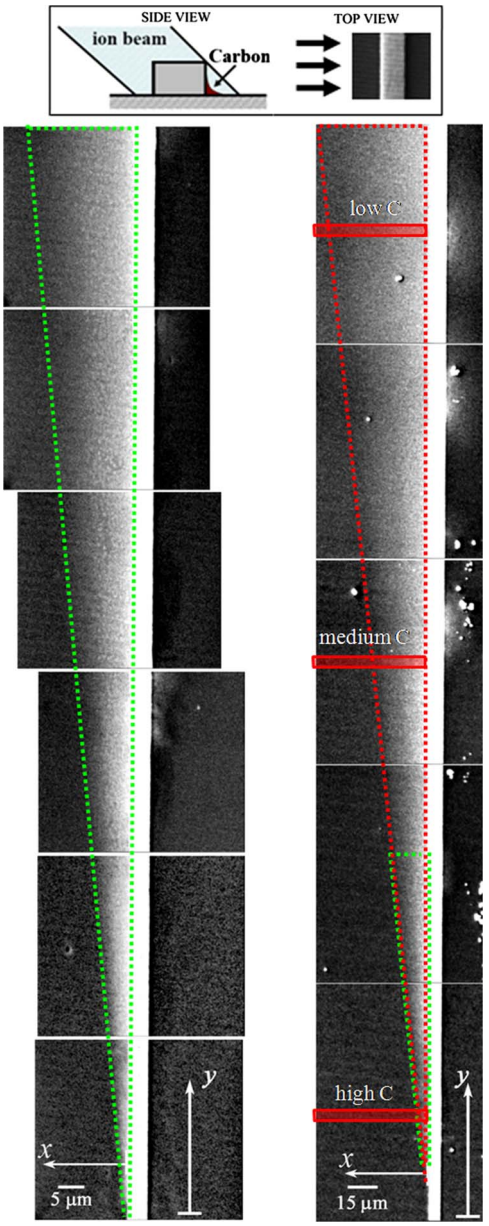

FIG. 3. (Color online) Diffusion regions for two different stripes after annealing for 10 min at 600 °C in presence of a wedged C coverage. Transversal sputtering has been used in this case (see inset on top). For both stripes, in the C-rich region (at the bottom) the diffusion is inhibited, while in the C-free region (at the top) the diffusion is favored with a continuous transition between these two extremes. The limit of the diffusion region as a function of the carbon coverage is outlined by the green contour (left panel) and red contour (right panel, where the rescaled green contour is also reported as a comparison). The regions with low, medium, and high C coverage used in Sec. III C are shown by red shaded areas.

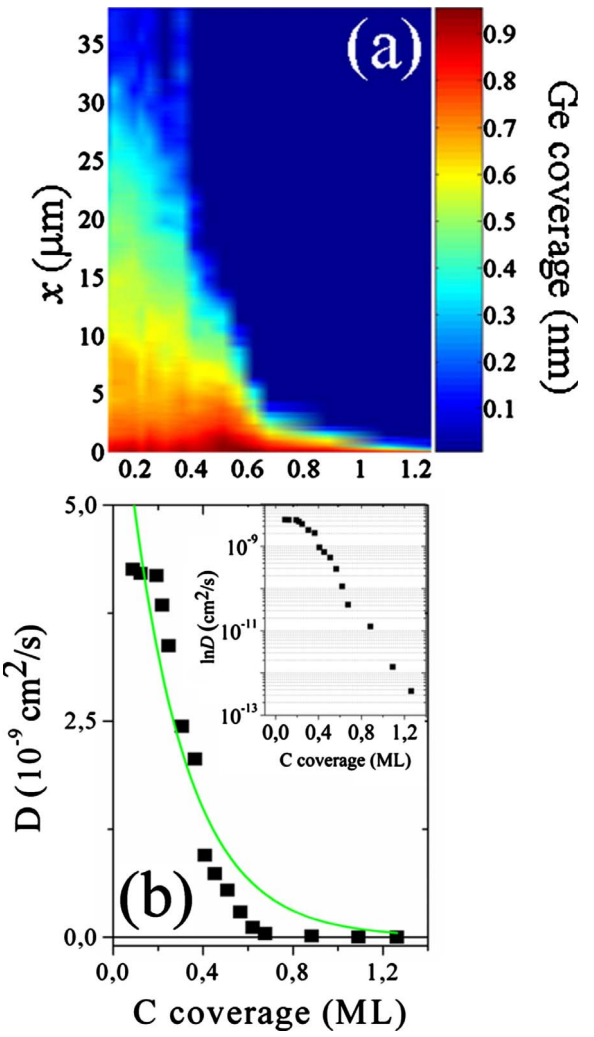

FIG. 4. (Color online) (a) Auger mapping of the Ge diffusion profiles as a function of the C coverage. (b) Quantitative correlation between the Ge diffusion coefficient and the carbon coverage (linear plot): the green continuous line is the best fit of the experimental data (black squares) using a model where the activation energy for surface diffusion linearly depends on the carbon coverage (see text). The free parameters D_0^* and E_A^1 result from the fitting to be $5.68 \pm 0.33 \times 10^{-2}$ cm^2/s and 0.29 ± 0.04 eV, respectively. Inset: logarithmic plot of the diffusion coefficient vs the carbon coverage.

function of y has been determined by measuring the C KLL Auger line [kinetic energy of 270 eV and IMFP of 1 nm (Ref. 36)]. Then its intensity variation has been fitted with a discrete layer model[35] similar to the one used for Ge in the previous section, where C is considered to be at the topmost of the surface. This is supported by the fact that for coverage greater than 0.2 ML carbon is preferentially found at surface sites.[40] Figure 3 shows the diffusion region for two different stripes after annealing for 10 min at 600 °C, where the modulation of the carbon coverage goes from the top (C-free) to the bottom (C-rich) of the figure. The effect of the carbon coverage on the Ge diffusion is dramatic: (i) the diffusion is fully inhibited on the right side of the stripes due to its shadowing effect on the ion beam, which prevents the C removal from the Si surface; (ii) on the left side the diffusion is completely quenched when the coverage exceed a critical value (which is about 1 ML) while in the C-free region the diffusion is favored and a continuous variation in the diffusion length with the C coverage leads from one extreme to the other. This behavior experimentally confirms the crucial role played by carbon in determining the Ge atomic mobility on Si(100).

Spatially resolved Auger analysis allowed to obtain the Ge coverage profiles after annealing as a function of the distance from the stripe, x, for different pre-existing C thickness in the submolayer regime, whose complete mapping is shown in Fig. 4(a). For the determination of the coverage profiles we used the same model exploited in the C-free case. Then by applying again the 1D diffusion model already described, the diffusion length behavior can be extracted by the map of the diffusion profiles. The correlation between the diffusion coefficient and the C coverage, shown in Fig. 4(b), is finally obtained by the relation $L=2\sqrt{D\tau}$. We notice here that the analytical solution of the 1D diffusion model used in the case of C-*free* diffusion still represents a good approximation for the experimental behavior of the Ge coverage as a function of x. Although this model strictly applies only in case of perfect translational symmetry along the stripe, as in the C-free diffusion described in Sec. III A, it is still a good approximation in the present case: in fact the diffusion length varies slowly along the y direction from 0.35 to 30 μm over a 500 μm range (see right panel in Fig. 3). It is worth noting as well that by changing the C coverage from about 1 to 0.1 ML, a variation of about 4 orders of magnitude in the diffusion coefficient is obtained [see inset in Fig. 4(b)]. This experimentally shows the possibility to tune the surface diffusion of Ge by using a controlled coverage of carbon, opening interesting perspectives in technological applications and device fabrication.

We focus now on the discussion of the measured variation in the diffusion coefficient of Ge at 600 °C as a function of the carbon coverage in submonolayer regime. We show in Fig. 4(b) that the coefficient strongly decreases while increasing the surfactant coverage.

The reduction in the atomic mobility in presence of carbon has been generally related to the strong chemical interactions among Si, C, and Ge, and to the increment of surface roughness due to the C presence.[19–21] Moreover, the activation energies for the surface diffusion have been theoretically shown to strongly depend on the local strain field experienced by the diffusing atoms on the substrate surface along their diffusion pathway.[41–45]

We show here that a first-order expansion of the activation energy $E_A=E_A^0+E_A^1(\vartheta-\vartheta_0)$ as a function of the C coverage, ϑ (defined as the ratio between the thickness of the carbon layer as determined by the discrete layer model and the thickness of one monolayer in the C diamond crystalline structure), is enough to reproduce the gross features of the experimental dependence. The coverage threshold $\vartheta_0=0.16\pm0.06$ ML comes from the tendency of carbon to intermix with Si into the shallow layers of the substrate rather than stay at the surface. This will be extensively discussed later on in this section while the determination of ϑ_0 will be described in Sec. III C. The diffusion coefficient results accordingly

$$D(\vartheta,T)=D_0^*\exp\left(-\frac{E_A^0}{K_BT}\right)\exp\left[-\frac{E_A^1}{K_BT}(\vartheta-\vartheta_0)\right], \quad (5)$$

where the pre-exponential factor, D_0^*, represents an average effective value of the diffusion constant in presence of a carbon coverage.

The main panel in Fig. 4(b) shows the best fit of the experimental data using Eq. (5), where E_A^0 was set to the value found in the case of C-free diffusion, and D_0^* and E_A^1 have been considered as free parameter, resulting to be $5.68\pm0.33\times10^{-2}$ cm^2/s (the same as in the case of C-free diffusion within the experimental uncertainty) and 0.29 ± 0.04 eV, respectively.

On the basis of the experimental results reported here, we are not able to identify quantitatively a predominant factor among the chemical interactions, the surface roughness, and the strain field determining the reduction in the Ge atomic mobility. However, combining our observations with well-established results from the literature we propose that the most reasonable picture of the experiment is the diffusion of a SiGe top 1ayer with high Ge concentration ($\approx$80%) on a rough and compressively strained substrate surface. This scenario is discussed in the following paragraphs.

The increase in surface roughness with the carbon coverage can be induced by the tendency of C atoms to diffuse into the Si substrate.[46,47] In fact, the C incorporation in Si is essentially driven by the competition between the tendency of C atoms to occupy favorable sites and the minimization of the lattice elastic energy associated with the $c(4\times4)$ reconstruction strain field.[40] This process can result in the formation of separated reconstruction domains and in the increase of the roughness. Torigoe *et al.*[48] gave experimental and theoretical evidence for a monotonic dependence of the activation energy for surface diffusion by the surface roughness, which is shown to increase for higher carbon coverage at a Si surface. We measured by AFM the postannealing surface rms roughness, which increases with the C coverage from 0.20 ± 0.04 nm in the C-free regions up to 0.35 ± 0.05 nm in the C-rich regions. Thus the roughness seems to play a role in the observed variation in the diffusion parameters.

In the case of further coverage with Ge as in our experiment, we have to take into account the existence of a strong repulsive chemical interaction between Ge and C atoms, which has been both theoretically predicted[15,47] and experimentally demonstrated.[26] This interaction is able to force C into the shallow layers[16] where it is principally incorporated substitutionally,[49] forming stable Si-C bonds and giving rise to a strong compressive strain field. This C-induced strain field increases with the carbon content at the surface[16] and can be obtained at the first order within the Vegard law as being proportional to the carbon coverage. The enhancement of compressive strain of the substrate has been shown[41–44,50] to be responsible for an increase in the surface-diffusion energy barrier leading to a decrease in the mobility. Huang *et al.*,[43,44] based on first-principles calculations, found a linear correlation between this diffusion energy barrier and the substrate strain field.

Thus we propose a scenario where the decrease in the Ge diffusion coefficient between the C-free and the C-covered Si(100) substrate originates from the modulation of the activation energy induced by two contribution: (1) the roughness at the interface and (2) the increased compressive strain within the substrate. Both contributions determine a linear dependence of the activation energy, thus they are both described by the coefficient E_A^1 in the exponential factor of Eq. (5).

The fitting in Fig. 4(b) reveals that the Ge diffusion constant, $D_0^*=5.68\times10^{-2}$ cm^2/s, does not significantly change with respect to the C-free case, $D_0=6.08\times10^{-2}$ cm^2/s, showing that the main cause of the strong dependence of the diffusion coefficient from the C coverage comes from the activation energy.

The above discussion shows that Si-C bonds influence deeply the SiGe diffusion in our experiment so that the value of E_A^1 estimated here cannot be directly compared to the theoretical calculations of the diffusion on externally strained pure Si substrates. However, a qualitative explanation of the main trends is possible within the approximation that E_A^1 is determined only by the C-induced strain field. This needs to account for the real strain field induced by C atoms in the surface layer, whose determination requires the knowledge of the carbon concentration in the topmost layer. This issue will be properly addressed in the following discussion about the island self-assembly (Sec. III C), and thus the reader is referred there also for the discussion about the term E_A^1.

These results should be considered as a preliminary attempt to have a deeper insight in the comprehension of the processes governing the C-induced modulation of the atomic mobility. They give an experimental basis on both the identification of the factors influencing the surface diffusion and the quantitative prediction of the C-induced trend for the activation energy and the diffusion constant. We hope that these systematic results will motivate further experimental and theoretical works.

C. SiGe islands nucleation

During the annealing process, SiGe islands have spontaneously nucleated in the diffusion area over the continuous overlayer created by the diffusive motion of Ge atoms from the stripe (insets of Fig. 6). In the case of a clean Si(100) surface, the growth mode of the SiGe islands is SK (Ref. 51) in the whole range of temperature over which the nucleation is observed. In the initial phase of the SK growth a 2D flat SiGe wetting layer (WL) is formed, and the 3D island nucleation takes place only above a critical WL thickness.

We have investigated the island growth mode in presence of carbon acting as a surfactant. The critical overlayer thickness for the setting up of island nucleation has been determined as a function of the carbon coverage by coupling SAM analysis (giving both C coverage and OL thickness as a function of x and y) and AFM analysis (giving the density of the islands as a function of x and y). In the following we identify this critical thickness with the largest thickness of the OL at which the island density goes to zero (see Fig. 5). We found that this critical thickness varies from 0.8 ± 0.17 ML for a pre-existing C coverage of ~0.7 ML (identified in Fig. 3 as the C-rich region of the sample) to 1.8 ± 0.25 ML at ~0.4 ML C coverage (hereafter called intermediate C-coverage region), up to 3 ± 0.21 ML for ~0.2 ML C coverage (the low C-coverage region); the absolute uncertainty for the C coverage is about ±0.1 ML. The main source of uncertainty on the critical thickness is the intrinsic error in the thickness determination as obtained within the discrete layer model presented in Sec. III A. The error on the critical thickness value coming from the uncertainty on the onset position for island nucleation (see Fig. 5) is substantially negligible with respect to the one introduced by the model.

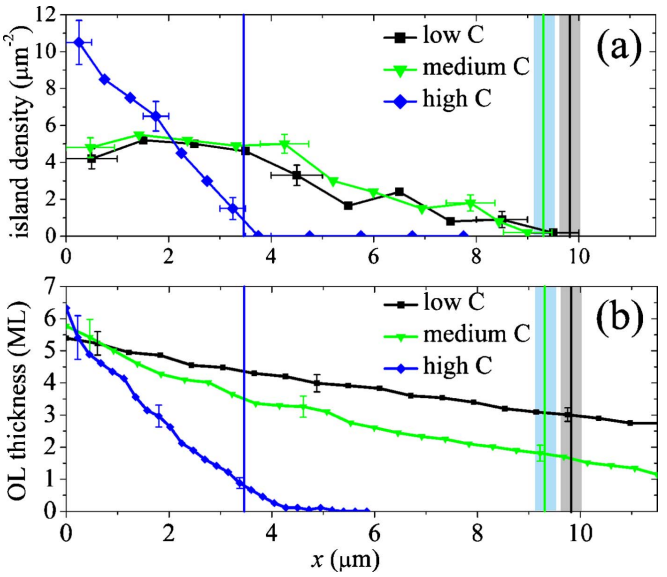

FIG. 5. (Color online) (a) Island density and (b) overlayer thickness vs distance, x, from the stripe in regions with different C coverages. The vertical blue, green, and black solid lines are the position of the onset for island nucleation in case of low C, medium C, and high C coverages, respectively (gray shaded zones represent the uncertainty). The comparison of the two graphs allows for the direct experimental determination of the critical OL thickness for nucleation with different C coverages.

In the low and intermediate carbon coverage regions, the measure confirms the SK growth mode observed in case of absence of surfactant, where the island formation is driven by elastic strain relaxation.[51] Since the surface energy of Si is larger than that of Ge, in the initial phase of the growth the Ge wets the Si substrate forming a uniformly strained SiGe film. The formation of an island can result in a reduction in the elastic energy stored in the overlayer and in the underlying Si substrate due to the partial elastic strain relaxation by the outward bending of the lattice planes. This mechanism becomes advantageous when the reduction in the elastic energy exceeds the increment of surface energy required by the larger surface developed by the island. This happens above a critical thickness of Ge coverage, after which the system spontaneously evolves toward the formation of 3D clusters.

In the high C-coverage region islands are able to nucleate even with a submonolayer Ge coverage. This observation is consistent with a Volmer-Weber (VW) growth mode,[26] where the formation of a larger Ge surface for a 3D island is energetically more convenient with respect to the accumulation of strain energy due to the formation of a continuous epitaxial layer. We attribute the reaching of this condition to the presence of a carbon-induced local compressive strain field.[20] In fact C atoms incorporate into the shallow volume of the Si substrate (as discussed in Sec. III B), thus reducing the lattice constant of the C alloyed Si surface due to their smaller size with respect to Si atoms and exaggerating the mismatch with the SiGe overlayer.

The monotonic dependence of the critical thickness on the C coverage can be used to gain a quantitative estimation of the C incorporation inside the Si substrate and improve the understanding of the interplay of the diffusion and nucleation properties. The simplified scenario is the following: as discussed above, the SiGe overlayer diffuses over a Si surface partially alloyed with carbon; the alloying increases the misfit strain between the SiGe thin film and the topmost layer of the substrate, thus increasing the amount of the elastic energy stored in the OL and consequently promoting the island nucleation at lower OL thicknesses.

We now propose a semiquantitative estimation of the carbon incorporation into the first layer of the Si substrate. The critical thickness at the 2D-3D transition corresponds to the minimization of the total free energy, F, of the system, which at first approximation can be obtained by considering only the contributions of the surface energy of the SiGe overlayer, γ, and of the elastic energy, E_{el}, stored in it[18]

$$F = \gamma + E_{el}.$$

The elastic energy E_{el} stored per unit area in the SiGe overlayer can be determined using the classical equation

$$E_{el} = 2\mu \frac{1+\nu}{1-\nu} \varepsilon^2 h, \tag{6}$$

where μ and ν are the shear modulus and the Poisson's ratio of the overlayer, ε is the misfit strain of a SiGe thin film on a Si-C alloy layer, and h is the OL thickness.

We point out that the surface energy of the SiGe overlayer, γ, can be considered at first approximation independent from the carbon coverage of the surface: in fact, the repulsive interaction between Ge and C forces C to be incorporated in subsurface sites and thus leaves unmodified the top surface of the SiGe overlayer. As a consequence at the critical thickness the reduction in the elastic energy stored in the overlayer for the case of nucleation on C-free and carbon covered regions is the same[18] and we can write

$$\varepsilon^2 h_{crit} = \varepsilon_0^2 h_0 \tag{7}$$

where $h_0 \sim 3.5$ ML (Ref. 52) and ε_0 are the critical thickness and the misfit strain in case of absence of carbon while h_{crit} and ε are the similar quantities for the C-covered Si surface. Equation (7) is valid in hypothesis that 3D clusters formed at the 2D-3D transition have the same morphological structure in both cases. The misfit strain ε and ε_0 depend at the first approximation only on the lattice parameters of the substrate and of the OL

$$\varepsilon = \frac{a_{\mathrm{SiGe}} - a_{\mathrm{SiC}}}{a_{\mathrm{SiGe}}} \quad \text{and} \quad \varepsilon_0 = \frac{a_{\mathrm{SiGe}} - a_{\mathrm{Si}}}{a_{\mathrm{SiGe}}}, \tag{8}$$

where $a_{\mathrm{Si}}=5.43$ Å refer to Si bulk and $a_{\mathrm{SiGe}}=a_{\mathrm{Si}}(1-\alpha)+a_{\mathrm{Ge}}\alpha=5.60$ Å (with $a_{\mathrm{Ge}}=5.64$ Å and $\alpha=0.81$ from Sec. III A) is the $\mathrm{Si}_{1-\alpha}\mathrm{Ge}_{\alpha}$OL lattice parameter obeying a Vegard law. The parameter of the uppermost C alloyed Si layer of the substrate, $\mathrm{Si}_{1-c}\mathrm{C}_c$ (where the carbon concentration c in the uppermost layer has not to be confused with the carbon coverage), can be evaluated in agreement with theoretical[53] and experimental[54,55] studies as

$$a_{\mathrm{SiC}} = a_{\mathrm{Si}}(1-c) + a_{\mathrm{C}}c + c(1-c)\beta, \tag{9}$$

where $\beta=-0.64$ Å (Ref. 55) is the so-called bowing parameter and $a_{\mathrm{C}}=3.56$ Å the lattice parameter of C in its diamond allotropes.

Thus combining Eqs. (7)–(9) and using the experimentally measured critical overlayer thickness we can evaluate the carbon concentration, c, within the topmost substrate layer and compare them with the corresponding carbon coverage. As shown in Fig. 6(a), in the C-rich region c is found to be about 6.7% while at intermediate C coverage it becomes 2.5%, decreasing down to 0.5% in the low C-coverage region. The experimental data are well fitted by a linear behavior [green line in Fig. 6(a)], showing that under a critical C coverage $\vartheta_0=0.16\pm0.06$ ML the C concentration c of the surface layer becomes negligible. These results are consistent with the picture that for low C-coverage subsurface sites are more energetically stable for carbon and justify the term $(\vartheta-\vartheta_0)$ in the activation-energy expansion $E_A=E_A^0+E_A^1(\vartheta-\vartheta_0)$ for surface diffusion introduced in the Sec. III B. They also support experimentally the Monte Carlo simulations and the *ab initio* calculations by Remediakis *et al.*,[40] according to which the ratio of surface to subsurface C atoms increases monotonically with increasing C coverage and becomes greater than 1 for a carbon coverage of 0.17 ML.

We discuss now the value of the first-order coefficient $E_A^1 \sim 0.29$ eV in the linear expansion of the activation energy $E_A=E_A^0+E_A^1(\vartheta-\vartheta_0)$ used in Sec. III B to fit the experimental trend of the diffusion coefficient. Based on the carbon concentration in the topmost layer of the substrate as given above, we can compare the quantitative results of our fitting in Sec. III B with the values reported by Huang *et al.*[43] They found by first-principles calculations on a biaxially strained Si(100) surface that the activation energy, E_A, for surface diffusion of Ge has a linear dependence on the strain applied to the substrate, $\hat{\varepsilon}$: $E_A=E_A^0-\hat{E}_A^1\hat{\varepsilon}$. In our case, the intermixing with carbon induces a strain field $\hat{\varepsilon} \cong (a_{\mathrm{SiC}}-a_{\mathrm{Si}})/a_{\mathrm{Si}}$ in the topmost layer of the substrate (not to be confused with the strain in the overlayer ε), which we can suppose to have a similar effect on the Ge diffusion. A comparison between the two above expressions of the activation energy E_A yields to the following relation between the first-order coefficients $\hat{E}_A^1$ and E_A^1:

$$E_A^1(\vartheta-\vartheta_0) = -\hat{E}_A^1\hat{\varepsilon}. \tag{10}$$

Equation (9) can be now used to explicit in the Eq. (10) the lattice parameter a_{SiC} in the top substrate layer as a function of the carbon concentration c. Thus Eq. (10) gives

$$c = \left(\frac{a_{\mathrm{Si}}}{a_{\mathrm{Si}} - \beta - a_{\mathrm{C}}}\right)\frac{E_A^1}{\hat{E}_A^1}(\vartheta-\vartheta_0), \tag{11}$$

where the second-order term has been neglected because of the small values of c found above. We notice that, within this approximation, Eq. (11) show a linear dependence between the carbon concentration c in the topmost layer and the carbon coverage ϑ, consistently with our previous discussion. From the fitting in Fig. 6(a) and $E_A^1=0.29\pm0.04$ eV, we

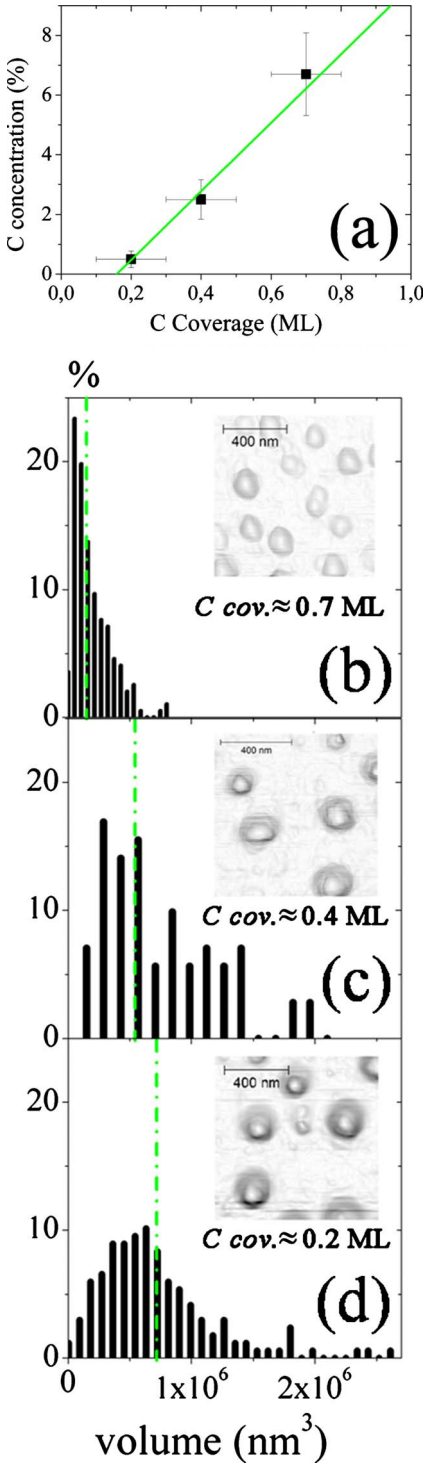

FIG. 6. (Color online) (a) Carbon concentration c (black squares) in the topmost layer of the C-alloyed Si substrate as a function of the C coverage ϑ; green line is the best linear fitting of the data. [(b)–(d)] Volume histograms of the SiGe islands nucleated in areas with different carbon coverages. Smaller islands are preferentially nucleated in the C-rich region [panel (b)] while bigger islands grow at low C-coverage zones [panels (c) and (d)]. The insets in the panels are AFM images in gradient modes of islands nucleated for different C coverages. The dashed-dotted green lines shown in each panel represent the average volume of the corresponding distribution.

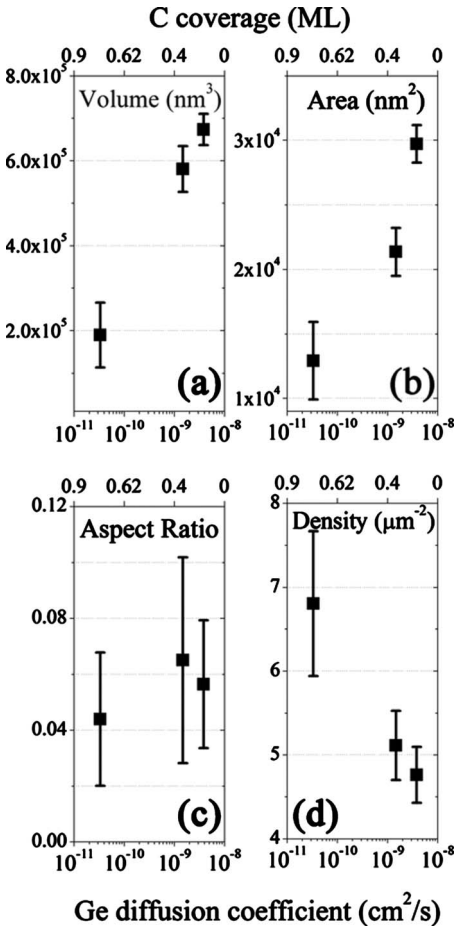

FIG. 7. Average (a) volume, (b) area, (c) aspect ratio, and (d) and density of the islands nucleated in areas with different C coverages correlated with the diffusion coefficient.

found $\hat{E}_A^1 = 5.45 \pm 1.32$ eV, to be compared with the values of 3.75 and 4.37 eV for perpendicular and parallel diffusion of Ge with respect to the dimer rows, respectively, found by Huang *et al.*[43] We attribute tentatively the larger value of $\hat{E}_A^1$ obtained here to the additional contribution of the C-induced surface roughness at the interface, which further increases the activation energy and consequently reduces the surface mobility.

In the following, we investigate the influence of carbon on the island size and density in order to understand the main factors governing the relative growth of individual self-assembled nanostructures. Figures 6(b)–6(d) show the volume distribution of islands nucleated in zones with a different carbon coverage and within a spatial region comprised between the stripe edge and a distance, x, from the stripe equal to about 3 μm. Such histograms show that smaller islands are preferentially nucleated in the C-rich region while bigger islands tend to grow where the C coverage is reduced. The spread of the distribution is also seen to increase for lower C coverage. By using the statistical analysis of the AFM data coupled with the SAM observations, the average size and the areal density of islands nucleated in regions with different C coverage are correlated with the diffusion coefficient showing a monotonic dependence, as reported in Figs.

7(a)–7(d). These results show that increasing the surface atomic mobility leads to the enhancement of volume and area of the islands, and a correspondent decreasing of the areal density while the aspect ratio remains almost constant. This behavior is in good agreement with the results reported by different authors using MBE,[29,31] showing that the deposition of submonolayer carbon enables the growth of smaller islands with higher density. The dependence of islands size and density as a function of the atomic mobility is qualitatively similar to the effect of a decreasing temperature in absence of surfactant.[56] The same trend is also seen when Sb is used as a surfactant at a fixed temperature,[57] even if different mechanisms dominate at atomic level with respect to a C surfactant due to the diverse nature of the chemical interactions Ge-C and Ge-Sb. Based on this observation and on the conclusion of the preceding Sec. III B, we attribute the size and density dependence of the nucleated islands from the carbon surfactant coverage to the C-induced modulation of the atomic mobility of Ge atoms on the surface. This is consistent with a diffusive origin of the growth process,[58] where diffusing atoms tend to be captured by the closest nuclei, and the islands grow by gathering mass essentially from a defined surrounding area. Our educated guess implies that the growth process should be well described by geometrical based models,[59,60] in particular by the Mulheran *capture zone model*,[61,62] and the island growth should be essentially controlled by the local kinetics of diffusion which determines the island density and governs the competition among the nuclei to collect Ge and Si in their surroundings. The experimental verification of the validity of the Mulheran model and of the deviations from its predictions overcomes the statistical certainty attainable within the present study and is left for future investigation.

IV. CONCLUSIONS

We have investigated the surface diffusion and the island nucleation of Ge on a C-covered Si(100) surface by scanning Auger microscopy and atomic force microscopy. First, the temperature dependence of Ge diffusion coefficient on a microscopic scale has been directly measured in case of a C-free Si surface, interpreting the results within a one-dimensional diffusion model. Then, the Ge diffusion coefficient at 600 °C has been monitored as a function of the carbon coverage, exploiting a continuous spatial modulation obtained by ion sputtering a homogeneous carbon layer during an increasing time. The increase in the carbon coverage from 0.1 to 1 ML, corresponds to a decrease in the diffusion coefficient from $\sim 3\times 10^{-9}$ to $\sim 3\times 10^{-13}$ cm^2/s. This huge dependence is discussed within a physical scenario where carbon is incorporated within the shallow volume of the Si substrate inducing a surface roughness and a compressive local strain field. These two phenomena, together with the chemical interactions among Si, C, and Ge are the main factors influencing the diffusion modulation and are described through a linear dependence of the diffusion activation energy on the C coverage.

Spontaneous nucleation of SiGe islands coexists with the continuous surface diffusion of Ge. By directly measuring the overlayer critical thickness for nucleation, we showed that the island growth mode gradually evolves from SK in case of absence of surfactant to VW for high surfactant coverage. This observation supports the possibility of engineering the self-assembly of SiGe islands by a controlled C deposition. A semiquantitative estimation of the C incorporation inside the Si substrate is then deduced from the experimentally measured monotonic dependence of the critical thickness on the C coverage. The carbon concentration inside the topmost Si substrate layer is found to increase linearly as a function of the carbon coverage, starting from a critical threshold $\vartheta_0=0.16\pm 0.06$ ML. Below this critical coverage, there is no sizable effect on the diffusion of Ge or on the nucleation of SiGe islands.

Finally, size and density of the spontaneously nucleated SiGe islands have been monitored in areas with different carbon coverages. The reduction in the surface atomic mobility with the C coverage leads to a decrease in the average size of the islands and a correspondent increase in the areal density. This trend is primarily interpreted within a capture zone model, where kinetic factors predominate.

ACKNOWLEDGMENT

This work was supported by the CARIPLO Foundation through the MANDIS Project.

[1] J. Drucker and S. Chaparro, Appl. Phys. Lett. **71**, 614 (1997).
[2] T. I. Kamins and R. S. Williams, Appl. Phys. Lett. **71**, 1201 (1997).
[3] O. Schmidt, C. Lange, K. Eberl, O. Kienzle, and F. Ernst, Appl. Phys. Lett. **71**, 2340 (1997).
[4] Y. W. Mo and M. G. Lagally, Surf. Sci. **248**, 313 (1991).
[5] A. E. Dolbak and B. Z. Olshanetsky, Cent. Eur. J. Phys. **4**, 310 (2006).
[6] T. Schwarz-Selinger, Y. L. Foo, D. G. Cahill, and J. E. Greene, Phys. Rev. B **65**, 125317 (2002).
[7] H. J. Kim, Z. M. Zhao, J. Liu, V. Ozolins, J. Y. Chang, and Y. H. Xie, J. Appl. Phys. **95**, 6065 (2004).
[8] C. Roland and G. H. Gilmer, Phys. Rev. B **47**, 16286 (1993).
[9] D. Srivastava and B. J. Garrison, Phys. Rev. B **46**, 1472 (1992).
[10] V. Milman, D. E. Jesson, S. J. Pennycook, M. C. Payne, M. H. Lee, and I. Stich, Phys. Rev. B **50**, 2663 (1994).
[11] M. Copel, M. C. Reuter, E. Kaxiras, and R. M. Tromp, Phys. Rev. Lett. **63**, 632 (1989).
[12] M. Copel, M. C. Reuter, M. Horn von Hoegen, and R. M. Tromp, Phys. Rev. B **42**, 11682 (1990).
[13] R. D. Bringans, R. I. G. Uhrberg, M. A. Olmstead, and R. Z. Bachrach, Phys. Rev. B **34**, 7447 (1986).
[14] R. M. Tromp and M. C. Reuter, Phys. Rev. Lett. **68**, 954 (1992).
[15] P. C. Kelires, Phys. Rev. Lett. **75**, 1114 (1995); Int. J. Mod.

Phys. C **9**, 357 (1998).
[16] G. Hadjisavvas, Ph. Sonnet, and P. C. Kelires, Phys. Rev. B **67**, 241302(R) (2003).
[17] D. J. Eaglesham, F. C. Unterwald, and D. C. Jacobson, Phys. Rev. Lett. **70**, 966 (1993).
[18] A. Portavoce, I. Berbezier, and A. Ronda, Phys. Rev. B **69**, 155416 (2004).
[19] O. Schmidt, S. Schieker, K. Eberl, O. Kienzle, and F. Ernst, Appl. Phys. Lett. **73**, 659 (1998).
[20] O. Leifeld, E. Muller, D. Grutzmacher, B. Muller, and K. Kern, Appl. Phys. Lett. **74**, 994 (1999).
[21] O. Leifeld, R. Hartmann, E. Muller, E. Kaxiras, K. Kern, and D. Grutzmacher, Nanotechnology **10**, 122 (1999).
[22] A. Beyer, E. Muller, H. Sigg, S. Stutz, D. Grutzmacher, O. Leifeld, and K. Ensslin, Appl. Phys. Lett. **77**, 3218 (2000).
[23] D. Dentel, J. L. Bischoff, L. Kubler, M. Stoffel, and G. Castelein, J. Appl. Phys. **93**, 5069 (2003).
[24] J. Stangl, V. Holy, and G. Bauer, Rev. Mod. Phys. **76**, 725 (2004).
[25] M. Stoffel, L. Simon, J. L. Bischoff, D. Aubel, L. Kubler, and G. Costelein, Thin Solid Films **380**, 32 (2000).
[26] O. Leifeld, A. Beyer, D. Grutzmacher, and K. Kern, Phys. Rev. B **66**, 125312 (2002).
[27] A. Bernardi, M. I. Alonso, A. R. Goñi, J. O. Ossó, and M. Garriga, Surf. Sci. **601**, 2783 (2007).
[28] A. Bernardi, M. I. Alonso, A. R. Goñi, J. O. Ossó, and M. Garriga, Appl. Phys. Lett. **89**, 101921 (2006).
[29] J. Y. Kim, S. H. Ihm, J. H. Seok, C. H. Lee, Y. H. Lee, E.-K. Suh, and H. J. Lee, Thin Solid Films **369**, 96 (2000).
[30] Y. Wakayama, L. V. Sokolov, N. Zakharov, P. Werner, and U. Gosele, J. Appl. Phys. **93**, 765 (2003).
[31] Y. Wakayama, G. Gerth, P. Werner, U. Gosele, and L. V. Sokolov, Appl. Phys. Lett. **77**, 2328 (2000).
[32] G. Isella, D. Chrastina, B. Rössner, T. Hackbarth, H.-J. Herzog, U. König, and H. von Känel, Solid-State Electron. **48**, 1317 (2004).
[33] N. Watanabe, S. Yamahata, and T. Kobayashi, J. Cryst. Growth **200**, 599 (1999); T. Hallam, F. J. Rueß, N. J. Curson, K. E. J. Goh, L. Oberbeck, M. Y. Simmons, and R. G. Clark, Appl. Phys. Lett. **86**, 143116 (2005).
[34] WSXM [I. Horcas, R. Fernández, J. M. Gómez-Rodríguez, J. Colchero, J. Gómez-Herrero, and A. M. Baro, Rev. Sci. Instrum. **78**, 013705 (2007)]; GWYDDION (http://gwyddion.net/).
[35] C. S. Fadley, Prog. Surf. Sci. **16**, 275 (1984).
[36] S. Tanuma, C. J. Powell, and D. R. Penn, Surf. Interface Anal. **21**, 165 (1994).
[37] M. Brehm, M. Grydlik, H. Lichtenberger, T. Fromherz, N. Hrauda, W. Jantsch, F. Schäffler, and G. Bauer, Appl. Phys. Lett. **93**, 121901 (2008).
[38] B. Tuck, *Atomic Diffusion in III-V Semiconductors* (Hilger, Bristol, 1988), Chap. 22, pp. 11–20.
[39] G. Medeiros-Ribeiro, A. M. Bratkovski, T. I. Kamins, D. A. A. Ohlberg, and R. S. Williams, Science **279**, 353 (1998).
[40] I. N. Remediakis, E. Kaxiras, and P. C. Kelires, Phys. Rev. Lett. **86**, 4556 (2001).
[41] D. J. Shu, F. Liu, and X. G. Gong, Phys. Rev. B **64**, 245410 (2001).
[42] A. van de Walle, M. Asta, and P. W. Voorhees, Phys. Rev. B **67**, 041308(R) (2003).
[43] L. Huang, F. Liu, and X. G. Gong, Phys. Rev. B **70**, 155320 (2004).
[44] L. Huang, F. Liu, G.-H. Lu, and X. G. Gong, Phys. Rev. Lett. **96**, 016103 (2006).
[45] R. Grima, J. DeGraffenreid, and J. A. Venables, Phys. Rev. B **76**, 233405 (2007).
[46] J. Tersoff, Phys. Rev. Lett. **74**, 5080 (1995).
[47] P. C. Kelires, Surf. Sci. **418**, L62 (1998).
[48] K. Torigoe, Y. Ohno, H. Kohno, T. Ichihashi, and S. Takeda, Surf. Sci. **601**, 5103 (2007).
[49] S. C. Jain, H. J. Osten, B. Dietrich, and H. Rucker, Semicond. Sci. Technol. **10**, 1289 (1995).
[50] V. Cherepanov and B. Voigtlander, Phys. Rev. B **69**, 125331 (2004).
[51] Y.-W. Mo, D. E. Savage, B. S. Swartzentruber, and M. G. Lagally, Phys. Rev. Lett. **65**, 1020 (1990).
[52] Tagliaferri, G. M. Vanacore, M. Zani, J. Osmond, and G. Isella (unpublished).
[53] P. C. Kelires, Phys. Rev. B **55**, 8784 (1997).
[54] M. Berti, D. De Salvador, A. V. Drigo, F. Romanato, J. Stangl, S. Zerlauth, F. Schaffler, and G. Bauer, Appl. Phys. Lett. **72**, 1602 (1998).
[55] D. De Salvador, M. Petrovich, M. Berti, F. Romanato, E. Napolitani, A. Drigo, J. Stangl, S. Zerlauth, M. Muhlberger, F. Schaffler, G. Bauer, and P. C. Kelires, Phys. Rev. B **61**, 13005 (2000).
[56] V. G. Dubrovskii, G. E. Cirlin, Yu. G. Musikhin, Yu. B. Samsonenko, A. A. Tonkikh, N. K. Polyakov, V. A. Egorov, A. F. Tsatsul'nikov, N. A. Krizhanovskaya, V. M. Ustinov, and P. Werner, J. Cryst. Growth **267**, 47 (2004).
[57] G. E. Cirlin, V. G. Dubrovskii, A. A. Tonkikh, N. V. Sibirev, V. M. Ustinov, and P. Werner, Semiconductors **39**, 547 (2005).
[58] M. Brinkmann, S. Graff, and F. Biscarini, Phys. Rev. B **66**, 165430 (2002).
[59] M. Li, M. C. Bartelt, and J. W. Evans, Phys. Rev. B **68**, 121401(R) (2003).
[60] J. G. Amar, M. N. Popescu, and F. Family, Surf. Sci. **491**, 239 (2001).
[61] P. A. Mulheran and J. A. Blackman, Phys. Rev. B **53**, 10261 (1996).
[62] S. Pratontep, M. Brinkmann, F. Nuesch, and L. Zuppiroli, Phys. Rev. B **69**, 165201 (2004).